

1 **Western Amazon was a center of Neotropical fish dispersal, as evidenced by the**
2 **continental-wide time-stratified biogeographic analysis of the hyper-diverse *Hypostomus***
3 **catfish**

4
5 Running title: Amazon is the center of fish dispersal

6
7 Luiz Jardim de Queiroz¹, Xavier Meyer², Yamila P. Cardoso³, Ilham A. Bahechar¹, Raphaël
8 Covain⁴, Thiago E. Parente⁵, Gislene Torrente-Vilara⁶, Paulo A. Buckup⁷, Juan I. Montoya-
9 Burgos¹

10
11 ¹ Department of Genetics and Evolution, University of Geneva, Switzerland

12 ² Department of Integrative Biology, University of California, Berkeley, USA

13 ³ Laboratorio de Sistemática y Biología Evolutiva. Facultad de Ciencias Naturales y Museo,
14 Universidad Nacional de La Plata. CONICET. Argentina

15 ⁴ Department of Herpetology and Ichthyology, Museum of Natural History of Geneva,
16 Switzerland

17 ⁵ Instituto Oswaldo Cruz, Fiocruz, Rio de Janeiro, Brazil

18 ⁶ Departamento de Ciências do Mar, Universidade Federal de São Paulo, Brazil

19 ⁷ Museu Nacional, Universidade Federal do Rio de Janeiro, Brazil

20 ⁸ iGE3 Institute of Genetics and Genomics of Geneva

21

22 Correspondence: Juan I. Montoya-Burgos. Department of Genetics and Evolution, Faculty of
23 Sciences, University of Geneva. Quai Ernest Ansermet 30, CH-1205 Geneva, Switzerland. E-
24 mail: Juan.Montoya@unige.ch.

25

26 **Abstract**

27 The Amazon is probably the most diverse realm on Earth, and is considered to be the primary
28 source of diversity and a center of dispersal for Neotropical terrestrial organisms. Yet, the
29 assumption that the Amazon basin is a primordial place of fish species origination and
30 dispersal into other drainages still need to be tested. We addressed this issue by inferring a
31 time-stratified biogeographic history and reconstructing the ancestral habitat preference of
32 *Hypostomus*, a continentally widespread and species-rich Neotropical genus. We found that
33 *Hypostomus* emerged in the Western Amazon (~14.7 Ma), when the Western Amazon River
34 was flowing northwards and disconnected from the Eastern Amazon. We show that dispersal
35 events in the first half of *Hypostomus* evolution occurred from the Western Amazon into
36 adjacent basins, initiating its Neotropical radiation. The ancestral preferred habitat consisted
37 in small rivers with running waters, a predominant habitat in river headwaters. Because of
38 strong niche conservatism in the early evolution of *Hypostomus*, we suggest that most of the
39 out-of-Western-Amazon dispersal occurred via headwater captures. The radiation of
40 *Hypostomus* was further promoted by major reconfigurations of river basins, which opened
41 dispersal opportunities into new drainages. Diversification in habitat preference coincided
42 with colonization of basins already occupied by congenics, indicative of niche shifts
43 triggered by inter-specific competition and species coexistence. By analyzing the evolutionary
44 history of *Hypostomus*, we show that Western Amazon was the main center of fish dispersal
45 in the Neotropical Region from Middle Miocene to the present, supporting the cradle
46 hypothesis of fish origination and dispersal.

47

48 **Keywords:** Amazon River, Lake Pebas, Biogeography, Ancestral ecology, Niche
49 conservatism

50 **Introduction**

51 The Neotropical Region, a large biogeographic realm that covers an area from
52 Southern Mexico to Argentina (Cox, 2001; Leroy et al., 2019), harbors a vast variety of
53 tropical biomes and habitats, and an unparalleled biotic diversity (Hughes, Pennington, &
54 Antonelli, 2013). The processes that have given rise to this diversity are complex, and the
55 many hypotheses of tempo and mode of diversification are still controversial (reviewed in
56 Antonelli, Ariza, et al., 2018). Yet, there is a consensus on the importance of the dynamic
57 geology and climatic variations in shaping the diversity observed nowadays (Antonelli, Ariza,
58 et al., 2018; Antonelli & Sanmartín, 2011). Therefore, taking these processes into account is
59 central for a better comprehension of the origin of the Neotropical biodiversity and the
60 geographical patterns of distribution.

61 One of the most striking features along the history of the Neotropical Region was the
62 uplift of the Andes, which was the result of a gradual thickening of the Earth's crust due to
63 the interaction between the Nazca and South American plates (Jordan et al., 1983; Pilger,
64 1984). The Andes is a continuous mountain range along the western edge of South America,
65 extending over more than 7,000 km in length. This mountain range has been uplifting slowly
66 over the last 30 million years, and the modern configuration and elevation were achieved
67 about 14–10 million years ago (Evenstar, Stuart, Hartley, & Tattitch, 2015; C. Hoorn et al.,
68 2010; Pilger, 1984). One of the most emblematic landscape reconfigurations driven by the
69 Andes uplift was the modification of the course of the Amazon River (C. Hoorn, Guerrero,
70 Sarmiento, & Lorente, 1995). Until around 10 Ma, the drainages of the current Amazon and
71 Orinoco rivers formed together the proto-Amazon-Orinoco system (PAO), which was the
72 most important basin that existed from the early Oligocene to the middle-Miocene in the
73 Neotropical Region. PAO flowed northwards into the Caribbean Sea through the outlet of the
74 contemporary Lake Maracaibo (C. Hoorn et al., 2010; Jaramillo et al., 2017). During the

75 Miocene, marine transgressions changed the landscape of part of the Neotropical Region,
76 including PAO, where a vast saline swamp-like environment was formed, the Pebasian Sea
77 (Wesselingh, Guerrero, Rasanen, Romero Pittman, & Vonhof, 2006). With the progressive
78 uplift of the Northern Andes, the outlet of PAO was gradually closed, blocking large masses
79 of water in the inland. Concomitantly, the rise of a topographic elevation in Northwestern
80 South America, the Vaupés Arch, caused the division of the POA into the western Amazonian
81 basin and the Orinoco basin (C. Hoorn et al., 2010). Then, with the breach of the Purus Arch,
82 which was the drainage divide separating current western and eastern Amazonian drainages,
83 the Amazon River eventually reached the Atlantic ocean and achieved its modern
84 configuration (James S. Albert et al., 2018; C. Hoorn et al., 1995; Carina Hoorn et al., 2017).

85 Following these drastic modifications of the Neotropical landscape during the
86 Miocene, Amazonian plant and animal lineages experienced an explosive diversification (C.
87 Hoorn et al., 2010). There is strong evidence that the Amazon region is likely the most
88 important source of diversity of terrestrial lineages worldwide (e.g. flowering plants, ferns,
89 birds, mammals and reptiles), playing a pivotal role in shaping the biodiversity across the
90 American continent (Antonelli, Zizka, et al., 2018; Musher, Ferreira, Auerbach, McKay, &
91 Cracraft, 2019). The reasons why Amazonia is a primary source of terrestrial biodiversity are
92 probably multiple, and some interdependent features have been evoked such as the high level
93 of environment heterogeneity spanning over a very large area, a dynamic landscape where
94 diversification has been kept at relatively high levels and constant over time, with low
95 extinction rates, and a high connectivity with neighboring biomes, facilitating dispersal of
96 terrestrial lineages (Musher et al., 2019).

97 As for fish, the Amazon Basin is the biogeographic core of the Neotropical system,
98 and by far the most species-rich river network (J. S. Albert & Reis, 2011; Böhlke et al., 1978),
99 with more than 7'000 species estimated (Lévêque, Oberdorff, Paugy, Stiassny, & Tedesco,

100 2008; Reis, Kullander, & Ferraris, 2003). The Amazon Basin has also been suggested to be a
101 cradle of fish diversity, an area where species have originated and immigrated into other
102 basins (J. S. Albert & Reis, 2011; James S. Albert et al., 2018; Fontenelle, Marques,
103 Kolmann, & Lovejoy, 2021; Oberdorff et al., 2019), but this hypothesis still needs further
104 testing. Whether the many and profound landscape changes that occurred in the Amazon
105 Basin were instrumental in fostering the origination, dispersal and diversification of modern
106 Neotropical fish lineages is an assumption that needs to be verified too.

107 The increasing knowledge about the historical modifications of Neotropical basins
108 offers a timely opportunity to infer freshwater fish ancestral distributions and dispersal routes
109 integrating the changes in watershed configurations through time, but this has been explicitly
110 explored in surprisingly few biogeographic reconstructions of Neotropical fish (e.g.
111 Fontenelle et al., 2021; Wendt, Silva, Malabarba, & Carvalho, 2019). To take advantage of
112 the accumulated knowledge of basins connectivity through time, it is important that
113 reconstructions use the finest possible biogeographic partitions of the hydrological systems,
114 but this implies extensive knowledge about species distribution as well as the inclusion of a
115 comprehensive taxonomic sampling. When based on a limited number of biogeographic
116 areas, as in most of the biogeographical studies of Neotropical fish (Mariguela, Roxo, Foresti,
117 & Oliveira, 2016; e.g. Roxo et al., 2014; Silva et al., 2016), ancestral distribution ranges tend
118 to be unrealistically large, some covering half of South America, thus losing credibility and
119 biological relevance.

120 In the present work, we investigated of the role played by the various Neotropical
121 river basins, integrating their historical changes in connectivity, as centers of origin and
122 diversification of new fish lineages and as dispersal platforms from which neighboring basins
123 were colonized. To this aim, we reconstructed the biogeographic history of one of the most
124 species-rich genera in the Neotropical Region, the armored catfish genus *Hypostomus*

125 (Loricariidae). *Hypostomus* are bottom-dwelling fishes with an herbivorous, detritivorous or
126 xylophagous diet, and are generally territorial and poor swimmers. By considering a large
127 fraction of the species diversity of this genus and by including representatives from most
128 South American drainages thanks to the comprehensive phylogeny of *Hypostomus* and
129 closely related genera we recently published [26], we assembled a dataset with one of the
130 finest geographical resolution to date, at the Neotropical level. To work efficiently at the
131 finest spatial resolution, we developed a new tool for the program RevBayes (Höhna et al.,
132 2016) which is an interactive environment for Bayesian statistical analyses with a
133 phylogenetic focus. The new tool we present here allows the user to disregard unrealistic
134 distribution ranges when performing biogeographic analyses, accelerating the analyses and
135 allowing the inclusion of more and finer geographical areas.

136 Taking advantage of our comprehensive dataset of the exceptionally diverse and
137 widespread genus *Hypostomus*, and using it a model Neotropical fish group, we tested
138 whether (i) the genus *Hypostomus* originated in the Amazon Basin, and (ii) the Amazon Basin
139 was the most important source of diversity for this lineage in the Neotropical Region.
140 Furthermore, we investigated how habitat preference evolved along the phylogeny of
141 *Hypostomus* and how it might have influenced the dispersal pattern of this genus across the
142 Neotropical river basins.

143 **Material and Methods**

144 *Phylogenetic reconstruction and tree calibration*

145 To reconstruct the phylogenetic tree of *Hypostomus*, we used the dataset published by
146 (Jardim de Queiroz et al., 2020), which includes six loci: the mitochondrial (i) Cytochrome c
147 oxidase subunit I protein-coding gene (*COI*) and (ii) *D-loop*, and the nuclear (iii) Gene
148 encoding Teneurin transmembrane protein 3 (*Hodz3*), (iv) a *Hypostomus* anonymous marker,

149 possible gene *ZBTB10* intron 3 (HAM-*ZBTB10-3*), (v) the *Recombination activating gene 1*
150 (*RAG1*) and (vi) the Fish *Reticulon 4* (*RTN4*). This dataset contained 206 *Hypostomus*
151 individuals organized in 108 putative species and 49 species belonging to closely related
152 genera (outgroups). We completed this dataset with three additional species: two samples of
153 *Hypostomus* sp. ‘Araguaia’ (Tocantins-Araguaia Basin, Brazil), one of *Hypostomus* sp.
154 ‘Aqua75’ (Paraguay River, Brazil) and one of *Hypostomus annectens* (Rio Dagua, a Pacific
155 coastal river of Colombia). The primers listed in (Jardim de Queiroz et al., 2020) were used to
156 amplify the desired six loci for the new samples. Genbank accession numbers of the
157 additional samples can be found in Supporting file 3 (Table S3).

158 The tree inference and calibration was performed using BEAST 1.8.1 (Drummond &
159 Rambaut, 2007), while the input file (an Extensible Markup Language, XML, file) was built
160 in BEAUTi 1 (Drummond, Suchard, Xie, & Rambaut, 2012a). We partitioned the data by
161 gene (six partitions), and substitution models and clock models were unlinked among the
162 partitions. A Yule process model was used as a species tree prior. We ran PartitionFinder 2
163 (Lanfear, Frandsen, Wright, Senfeld, & Calcott, 2016) to identify the best nucleotide
164 substitution model based on Bayesian information criterion (BIC): TRN+I+G for *COI* and *D-*
165 *loop*, HKY+G for *Hodz3* and HAM-*ZBTB10-3*, HKY+G+I for *RTN4*, and K80+G for *RAG1*.
166 For the six partitions, we assumed a lognormal relaxed clock (Drummond, Ho, Phillips, &
167 Rambaut, 2006) using a lognormal distribution model with log mean of 0.01 and log standard
168 deviation of 1. We ran five independent runs (15×10^7 generations), sampling the parameters
169 values and trees every 10,000 generations (Supporting file 1).

170 To time-calibrate the tree, we overcame the absence of *Hypostomus* fossils by
171 applying an approach based on biogeographic calibrations. Ho and colleagues (Ho et al.,
172 2015) listed two key assumptions for the application of such calibrations: i) a significant
173 impact on population or species, and ii) available information on the age. We used four dated

174 hydrogeological changes as calibration points that meet these assumptions: (1) Uplift of the
175 Cordillera de Mérida (mean age of $8.0 \text{ Ma} \pm 0.08$ at the crown age of *H. honda* + *H.*
176 *plecostomoides*); (2) Uplift of the Ecuadorian Andes ($10 \text{ Ma} \pm 0.07$ at the crown age of
177 *Aphanotorulus* + *Isorineloricaria*); (3) Disconnection of the Tocantins-Araguaia River from
178 the Amazon Basin ($2.6 \text{ Ma} \pm 1$ at the crown age of *Hypostomus* sp. ‘gr. *cochliodon*-Tar’ +
179 *Hypostomus* sp. ‘gr. *cochliodon*-Xin2’) (4) Boundary displacement between the Amazon and
180 the Rio Paraguay systems ($1 \text{ Ma} \pm 0.6$ at the crown age of *Hypostomus* sp. ‘Rio Grande’ +
181 *Hypostomus* sp. cf. *borelli*). For more details regarding the calibration points, refer to the
182 Supporting file 3. The inclusion of multiple calibrations may reduce the influence of eventual
183 erroneous calibration and improve the robustness of the time tree (Duchêne, Lanfear, & Ho,
184 2014).

185 To evaluate the effect of the use of the aforementioned biogeographic events as
186 calibration points in the *Hypostomus* time-tree, we performed three additional inferences
187 (Supporting file 1). In each of these new reconstructions, one of the new calibration points
188 was not used. We then assessed if important disparities in the time estimates among the
189 distinct reconstruction are observed. Furthermore, assuming that the use of calibration points
190 during phylogenetic reconstructions may improve accuracy of the phylogenetic
191 reconstructions (Drummond et al., 2006), we also verified if major changes in the topology of
192 the tree were observed. For these alternative time-tree reconstructions, we used the same
193 parameters and priors as described before.

194 *Ancestral distribution range*

195 To infer the biogeographic history of *Hypostomus*, we estimated the ancestral
196 distribution range of all the nodes of the phylogenetic tree using the Dispersal–Extinction–
197 Cladogenesis (DEC) model (Ree et al., 2005; Ree & Smith, 2008) implemented in RevBayes

198 (Höhna et al., 2016) (Supporting file 2). The DEC model was originally described — and has
199 been often used — as a maximum likelihood approach (Ree et al., 2005; Ree & Smith, 2008),
200 but RevBayes offers a Bayesian implementation, It allows one to assess parameter uncertainty
201 and to calculate Bayes Factor to compare competitive hypotheses (Landis, Freyman, &
202 Baldwin, 2018).

203 Discrete biogeographic regions (BHG) were defined based on the areas proposed
204 by Abell et al. (2008), and on the areas of Neotropical freshwater fish endemism (Hubert &
205 Renno, 2006; Montoya-Burgos, 2003; Vari, 1988). These areas were adapted to fit with the
206 BHG regions that remained unfragmented during the historical changes in basin connectivity
207 from the Miocene to the present. In this way, we defined 12 BHG regions (Figure 7A): (BHG
208 region A) *Western Amazon* covers the upper portion of the Amazon Basin to the Middle
209 Amazon River, including the sub-basins of Madeira and Negro rivers; (B) *Eastern Amazon*
210 includes the lower portion of the Amazon River and tributaries draining in the Guiana and
211 Brazilian shields, such as the Tapajós, Xingu and Trombetas rivers; (C) *Tocantins-Araguaia*
212 River Basin; (D) *Orinoco* River Basin and the island of Trinidad; (E) *Guianas–Essequibo*
213 includes the Guianese coastal rivers draining the Guyana Shield and flowing into the Atlantic
214 Ocean; (F) *Paraguay* River System covers the Pilcomayo and Paraguay rivers and the lower
215 section of the Paraná River; (G) *Upper Paraná* River covers the upper portion of the Paraná
216 River; (H) *Uruguay* River Basin and *Lagoa dos Patos* System; (I) *Coastal Atlantic* drainages
217 of the South- and Northeastern Brazil from the south of Santa Catarina state in Brazil to the,
218 but not including, São Francisco River mouth; (J) *São Francisco* River Basin; (K) *Coastal*
219 *Atlantic* drainages of Northern Brazil includes rivers flowing into the Atlantic Ocean between
220 the Tocantins-Araguaia and São Francisco mouths; (L) *trans-Andean* drainages includes the
221 Lake Maracaibo, Magdalena River Basin (which drain into the Caribbean Sea) and Pacific
222 drainages of Ecuador and Colombia.

223 We defined two stationary biogeographic models, with constant constraints in
224 dispersal possibilities for the complete time period of our study (25 Ma to present). The first
225 model (M1) assumes full permeability between all pairs of BHG regions (connectivity value =
226 1), irrespective of whether they are adjacent to each other or not. The second model (M2) is
227 semi-permeable, in which dispersion is possible but constrained between adjacent BHG
228 regions (connectivity value = 0.1), and dispersion is not allowed between non-adjacent BHG
229 regions (connectivity value = 0). One of the advantages of the DEC model is the possibility of
230 combining *a priori* different temporal connectivity patterns among BHG regions by using a
231 pairwise matrix of connectivity. Hence, we defined a third time-stratified model (M3) by
232 taking into account historical changes in connectivity across BHG regions. For this aim, we
233 used the following connectivity values: (i) a value of 1 was given to a pair of BHG regions for
234 the period of time in which they displayed a full hydrological continuity (i.e. they were parts
235 of a same basin); (ii) a value of 0.5 to a pair of BHG regions for the period of time in which
236 they displayed partial hydrological continuity, for example through a permanent local
237 connection such as the Casiquiare River currently connecting the Western Amazon with the
238 Orinoco basins; (iii) a value of 0.1 to a pair of adjacent BHG regions showing no particular
239 long standing water connection; and (iv) 0 to non adjacent BHG regions. We established these
240 rules because fish, being limited to the aquatic environment, cannot disperse from non-
241 adjacent regions in a single step. The M3 considered four time windows (Supporting file 3,
242 Table S2), each one with a determined connectivity matrix according to the known paleo-
243 landscape changes. For details, see Supporting file 3.

244 To run the time-stratified (M3) and stationary models (M1 and M2), we estimated a
245 single average value of allopatry and subset sympatry rates. Moreover, the maximum
246 ancestral range was set to three BHG regions, which corresponds to the maximum number of
247 regions occupied by extant *Hypostomus* species included in our study. The original functions

248 in RevBayes were originally designed to explore all the combinations of discrete BHG
249 regions (Höhna et al., 2016). In our case, with a total of 12 BHG regions and setting the limit
250 of ancestral areas to combinations of at most three BHG regions, we would have 298 possible
251 combinations to compute. To optimize the analyses and reduce computation time, we
252 modified the RevBayes script to disregard combinations of areas that have no biological
253 meaning in terms of species distribution range, such as very distant areas with no present or
254 past connectivity (e.g. *ABK*, *AGH* or *CDE*), reducing the number of possible ranges to 67.
255 This new feature was key to this study since the biogeographic analyses defined using default
256 RevBayes functionalities could not be successfully run for our dataset due to their excessive
257 computational cost (i.e., requiring more than 32GB of RAM and several minutes per
258 iteration). With our modification, the analyses did not suffer from memory limitations and ran
259 faster (i.e., 17 seconds per iteration). A version of the helper script for biogeographic
260 reconstructions in RevBayes can be found in the Supporting file 2 as well as in the GIT
261 repository <https://bitbucket.org/XavMeyer/biogeographyrevscript/src/master/>, where
262 improvements may be available. The results obtained with the different biogeographic
263 models were compared and ranked by calculating the Bayes Factor, which is a typical model
264 selection approach in the Bayesian framework (Baele, Lemey, & Vansteelandt, 2013). To do
265 so, we ran 40'000 iterations sampling every 10 iterations. Convergence was assessed by
266 plotting log parameters in Tracer.

267 *Habitat preference evolution*

268 In order to investigate how ancestral ecology played a role on the biogeographic
269 history of *Hypostomus*, we evaluated the pattern of evolution of the habitat preference across
270 the phylogenetic tree of *Hypostomus*. We reconstructed the ancestral habitat preference by

271 defining the nine categories of habitats that were modified from those according to (2011), as
272 listed below (Figure 6):

273 i) *Slow flowing small streams (SFSS)*: streams with maximum 50 m width, such as
274 headwater streams or small tributaries, being localized either in uplands or in lowlands,
275 generally muddy, with substrate comprising mostly of clay and sand.

276 ii) *Medium to fast flowing small streams (FFSS)*: as the previous category, but
277 substrate comprised mainly of rocks or small stones.

278 iii) *Slow flowing medium-sized rivers (SFMR)*: rivers with *c.* 50–1,000 m width, either
279 placed in uplands or lowlands, with muddy and/or sandy substrate.

280 iv) *Medium to fast flowing medium-sized rivers (FFMR)*: as in SFMR, but substrate
281 mainly composed of gravel, stones and rocks. Medium-sized rapids and waterfalls are
282 included in this category.

283 v) *Slow flowing large rivers (SFLR)*: large rivers with more than 1 km width, which
284 include all the rivers or portions of them with very slow flowing waters, with substrate
285 composed mainly of clay and sand.

286 vi) *Medium to fast flowing large rivers (FFLR)*: as in SFLR, but with gravel, rocky and
287 stony substrates, including large rapids and waterfalls.

288 vii) *Floodplains and ponds (FLPO)*: areas that are seasonally inundated by the main
289 rivers, including *várzea* and *igapó* lakes, ponds, flooded forests, flooded savannahs and
290 flooded grasslands.

291 viii) *Freshwater estuarine systems (FRES)*: areas of estuary of very large rivers, where
292 the salinity is still very low. In this category we included only the Río de La Plata,
293 comprising specifically the mouth of Uruguay and Paraguay rivers.

294 ix) *Brackish water* (BRWA): estuary and coastal regions characterized by relatively
295 high salinity. A single *Hypostomus* species lives in this very atypical habitat in the coast
296 of the Guyanas.

297 We used BEAST 1.8.1 (Drummond, Suchard, Xie, & Rambaut, 2012b) to reconstruct
298 the ancestral habitat state (Supporting file 1). We employed the aforementioned time-
299 calibrated tree, by fixing topology and branch lengths. We assumed a symmetric model for
300 discrete state reconstructions. A strict clock was used, thereby enforcing a homogeneous rate
301 of trait evolution across all branches, and the prior on mean rate of habitat evolution was set
302 as a gamma distribution. Three independent runs of 5×10^7 generations, sampled every
303 5,000th generation, were ran. Convergence of the runs and ESS >200 were confirmed with
304 Tracer 1.6. The post-burn-in samples from the three runs were combined using LogCombiner
305 2.4.8 to produce a consensus tree in TreeAnnotator 2.4.8.

306 **Results**

307 *A robust calibrated Phylogeny of Hypostomus*

308 We inferred a time-calibrated phylogeny of *Hypostomus* using four calibration points
309 (calibration scenario 1) indicating that the *Hypostomus* lineage trace back to 14.7 Ma (HPD
310 95% = 17.8–11.4 Ma), which corresponds to the split between *Hypostomus* and its closest
311 relatives *Hemiancistrus fuliginosus* + *Hemiancistrus punctulatus* (Figure 1). The estimated
312 age of the Most Recent Common Ancestor (MRCA) of *Hypostomus* is 12.1 Ma (14.3–10.1
313 Ma) while the ages of divergence between the main *Hypostomus* lineages are presented in our
314 calibrated phylogeny (Figure 1).

315 To evaluate the robustness of our calibrated phylogeny, we assessed the compatibility
316 of each calibration point with regards to the three others by running three new calibrated
317 phylogenetic inferences with the exclusion of one of the four calibrations at a time

318 (calibration scenarios 2 to 4 in Table 1). The resulting topologies were very similar among
319 each other and also with the results obtained with the full set of calibration points (Supporting
320 file 1). The super-groups of *Hypostomus*, as previously defined in the literature (Jardim de
321 Queiroz et al., 2020), were reconstructed with strong posterior probability ($PP \geq 0.97$) in all
322 calibration scenarios (Supporting file 1). The only noticeable difference was the age retrieved
323 for the calibration point 2 consisting in the split between *Isorineloricaria* and *Aphanotorulus*
324 (IA split) attributed to the uplift of the Ecuadorian Andes. When this calibration point was not
325 used as a prior (calibration scenario 4), the age of this split was estimated to be 19.6 Ma
326 (27.3–13 Ma), that is, older than the uplift of the Ecuadorian Andes, the hypothesized
327 vicariant event causing the split. We also noticed that the splitting ages at the deepest nodes
328 were in general more ancient when the IA split was not considered as a calibration point
329 (calibration scenario 4). However, in all these cases, there is an important overlap of the HPD
330 95% across the different calibration scenarios (Table 1). Therefore, we used the scenario with
331 four calibration points (calibration scenario 1) in the downstream analyses.

332 *Western Amazon was a centre of origin and dispersal*

333 We reconstructed the biogeographic history of the genus *Hypostomus* using three
334 biogeographic models in RevBayes. The first two were stationary models in which the
335 connectivity between biogeographic (BHG) regions remained unchanged along time: the
336 first with full permeability between all pairs of BHG regions (Model 1, M1), and the second
337 combining (i) limited permeability between adjacent BHG regions and (ii) no permeability
338 between non-adjacent ones (Model 2, M2). The third model (M3) assumed a time-stratified
339 scenario with connectivity patterns adapted to four time windows, which were defined based
340 on the most important hydrological changes documented for South America. The time-
341 stratified model M3 showed the highest score relative to the two stationary models (Bayes

342 Factor difference > 19; Supporting file 3, Table S1), providing the best approximation of
343 ancestral ranges throughout the radiation of *Hypostomus*, which we used in our further
344 analyses. Accordingly, the most recent common ancestor (MRCA) of the lineage comprising
345 *Hypostomus* and its sister *Hemiancistrus* group lived in the Western Amazon + Paraguay
346 (start state = region AF; posterior probability = 0.44; Supporting file 1a). This ancestor then
347 experienced a vicariant event (AF → A|F), by which the ancestral population isolated in the
348 Western Amazon (A) gave origin to the first ancestral *Hypostomus*. While living in Western
349 Amazon, this ancestral *Hypostomus* split into consecutive lineages being at the origin of the
350 four recognized super-groups of *Hypostomus* (*Hyp. cochliodon* super-group, *Hyp. hemiurus*
351 super-group, *Hyp. auroguttatus* super-group and *Hyp. plecostomus* super-group). The
352 divergences among these super-groups followed a pattern where one of the descendants
353 remained in Western Amazon, while its sister descendent colonized a new BHG region
354 (Figure 1). In this way, a population from Western Amazon colonized the Guianas–Essequibo
355 region (A → AE) giving rise to the ancestor of the *Hyp. hemiurus* super-group (HHsg).
356 Subsequently, stemming from the ancestral species that remained in Western Amazon, a
357 population entered into the Paraguay System (A → AF), initiating the *Hyp. nematopterus* +
358 *Hyp. auroguttatus* super-group (HASg). Finally, the ancestral species still residing in Western
359 Amazon gave rise to the *Hyp. plecostomus* super-group (HPsg).

360 Similarly, other Neotropical main basins were gradually colonized by *Hypostomus*
361 representatives stemming from Western Amazon. The first colonization of the Orinoco Basin
362 (BHG region D) took place around 10.5 Ma with the arrival from Western Amazon (A → D) of
363 the ancestor of *Hyp. sculpodon* (a member of the HCsg lineage; Figure 2). The Lower
364 Amazon Basin (Eastern Amazon, BHG region B) was also colonized first by emigrants
365 stemming from Western Amazon at 9.9 Ma (A → BC; Figure 2). The *trans*-Andean area (BHG
366 region L) was the only region adjacent to the Western Amazon that was not initially colonized

367 by Western Amazon ancestors, but by *Hypostomus* stemming from the Orinoco Basin (D →
368 DL; Figure 2).

369 According to our biogeographic reconstructions, the Lower Amazon Basin (BHG
370 region B), the Orinoco Basin (BHG region D), and the Guianas-Essequibo System (BHG
371 region E) were repeatedly colonized by *Hypostomus* species coming from Western Amazon.
372 For example, the Orinoco Basin was independently colonized by Western Amazon ancestors
373 at least in three instances: once in the lineage leading to *Hyp. hemicochliodon* (A→ABD; 1.3
374 Ma, Figure 2), once in the lineage leading to *Hyp. hondae* + *Hyp. plecostomoides* (A→AD;
375 8.8 Ma, Figure 2), and once at the root of the *Hyp. robinii* group (A→AD; 7.1 Ma, Figure 5).
376 The Guianas-Essequibo System, besides the early colonization by the ancestor of the HHsg,
377 was independently colonized two additional times by Western Amazon ancestors, the first
378 leading to the monotypic lineage of *Hyp. nematopterus* (A→E; 9.2 Ma, Figure 4) and the
379 second giving rise to the *Hyp. watwata* group (A→AE; 7.3 Ma, Figure 5). The re-colonization
380 of the Lower Amazon by Western Amazon emigrants can be exemplified by the arrival of the
381 ancestor of today's *Hyp.* sp. 'Paru' (A→AB; 5 Ma, Figure 3).

382 *Hypostomus* radiation into Southern and Eastern South American basins

383 The colonization of the Upper Paraná (region G) started with the ancestor of the HAsg
384 at 9.2 Ma (Figure 4), stemming from the pre-existing Paraguayan lineage (F→FG).
385 Subsequently, also within the HAsg, the first colonization of the Uruguay System/Lagoa dos
386 Patos (region H) took place at about 4.6 Ma, with colonists emigrating from the Paraguay
387 System (F→FH, Figure 4). Moreover, we recovered two independent colonization of the São
388 Francisco River (region J), both within the *Hyp. auroguttatus* super-group (HAsg). The first
389 gave origin to the *Hyp. asperatus* group (C→CJ; 6.4 Ma), while the second was the ancestor

390 of today's *Hyp.* sp. 'BR98751' (G→GJ; 1.9–1.4 Ma), a member of the *Hyp. regani* group
391 (Figure 4).

392 A single colonization of the coastal Atlantic drainages of Northern Brazil (region K)
393 was inferred and involved the ancestor of *Hyp. pusarum* + *Hyp.* sp. "Pindaré" (B→BCK; 4.2
394 Ma, Figure 5). On the other hand, the coastal Atlantic rivers (region I) were colonized four
395 independent times. In two cases the ancestral colonists stemmed from the Upper Paraná: (i)
396 the ancestor of *Hyp. auroguttatus* (belonging to the HAsg) at 5.7 Ma (G→I, Figure 4) and (ii)
397 the ancestor of *Hyp.* sp. "gr. *ancistroides* 4" (HPsg) (G→GI) at 3.6 Ma (Figure 5); while in
398 the third case (iii) the colonists came from a region composed of the Paraguay plus the Upper
399 Paraná, at about 3.2 Ma, which led to a small monophyletic lineage comprising five species of
400 our dataset, including *Hyp. affinis* and relatives (FG → GI, Figure 5); and in the fourth case
401 (iv) the ancestor stemmed from the São Francisco Basin at around 1.8 Ma and led to the
402 group of species *Hyp.* sp. "AZ4" + *Hyp.* sp. "Contas" + *Hyp.* aff. *francisci* (J→JI, Figure 4).

403 *Habitat preference conservatism with recent shifts*

404 The ancestral habitat preference reconstructed with BEAST revealed that the MRCA
405 of *Hypostomus* was living in small to medium size streams and rivers with medium–fast
406 flowing waters (EF, Figure 6). This type of habitat remained the preferred one along most of
407 the evolutionary history of the genus and still persists in many representatives of all main
408 lineages. This result is indicative of marked niche conservatism in this genus. Among the
409 changes in habitat preference, the most ancient shift is observed in the stem branch of the
410 lineage including *Hyp. hoplonites* + *Hyp. carinatus* about 7.9 Ma, as this lineage adapted to
411 more lentic environments (floodplains and slow flow medium-large rivers, ACD). The next
412 shift in habitat preference occurred at about 6.1 Ma within the HCsg lineage, with a change
413 towards more lentic environments (floodplains + slow flow medium–large rivers, ACD; and

414 floodplains + slow flow small–medium rivers, ABC). All the remaining shifts in habitat
415 preference occurred quite recently, starting at about 4.5 Ma. Today, the proportion of species
416 inhabiting lentic habitats is approximately equal to the proportion living in lotic habitats
417 (Figure 6).

418 **Discussion**

419 Although the Amazon region has been recognized as the major source of diversity of
420 terrestrial organisms in the Neotropical realm [e.g. 15, 16], an equivalent role for freshwater
421 lineages has not been thoroughly investigated. In the present study, we have addressed this
422 issue by analyzing *Hypostomus* as a model group due to its remarkable species-richness, its
423 continental-wide distribution, and because its species have colonized all Neotropical
424 freshwater habitats. We assembled information about the distribution, ecology and habitat
425 preference of 111 *Hypostomus* species from the main basins of South America and we
426 calibrated a large phylogenetic tree. We also took advantage of the growing knowledge
427 related to the history of river basins and landscape changes in Tropical South America (J. S.
428 Albert & Carvalho, 2011; J. S. Albert & Reis, 2011; Carvalho & Albert, 2011; e.g. C. Hoorn
429 et al., 2010; John G. Lundberg, Pérez, Dahdul, & Aguilera, 2011; Tagliacollo, Roxo, Duke-
430 Sylvester, Oliveira, & Albert, 2015) to define time windows for each configuration of river
431 network and connectivity, leading to more realistic biogeographic reconstructions. To
432 improve our biogeographic reconstructions, we developed a new tool for RevBayes allowing
433 for computationally tractable analyses with more precise geographic divisions by exploiting *a*
434 *priori* biologically meaningful distribution ranges.

435 *Western Amazon was the centre of origin of Hypostomus*

436 Deciphering the precise distribution range of a distant ancestor based on its current
437 day descendants depends largely on the completeness of the species sampling, the knowledge

438 of the species distribution range and the size and number of the geographic areas considered
439 in the analysis. Previous attempts to infer the ancestral range of *Hypostomus* used restricted
440 taxonomic sampling, and resulted in excessively large ancestral distribution range for the first
441 ancestral *Hypostomus*, encompassing the entire proto Amazon-Orinoco System (Cardoso et
442 al., 2021) or even the proto-Amazon-Orinoco plus Upper Paraná (Silva et al., 2016). With our
443 comprehensive taxonomic sampling of *Hypostomus* and close relatives, we found that the
444 MRCA of *Hypostomus* inhabited the Western Amazon, an area that nowadays corresponds to
445 the Upper Amazon Basin including some important tributaries, such as the Madeira, Negro,
446 Purus and Japurá rivers. Our calibrated phylogeny based on four cross-tested calibration
447 points (Figs. 1–5; Supporting file 1: Time tree 1) indicates that the first ancestral *Hypostomus*
448 emerged in the Middle-Miocene, approximately from 14.7 Ma, and started to diversify at
449 approximately 12.1 Ma. These temporal results are in agreement with previous hypotheses (J.
450 I. Montoya-Burgos, 2003; Silva et al., 2016), but contrast with the Oligo-Miocene origin (~25
451 Ma) proposed recently (Cardoso et al., 2021).

452 Our findings indicate that the first ancestral *Hypostomus* originated and lived in the
453 Western Amazon Region, at a time where this region was mostly occupied by the Lake Pebas.
454 This mega basin was composed of a mosaic of lentic water bodies and wetlands that
455 dominated the lowlands of western Amazonia, bordered by the slopes of the Andes on the
456 western side and of the Brazilian and Guyana shields on the eastern side (C. Hoorn et al.,
457 2010; Lovejoy, Bermingham, & Martin, 1998; Wesselingh et al., 2006).

458 Due to marine transgressions, the lentic waters of the Lake Pebas basin are suggested
459 to have been influenced by the sea, increasing its salinity (Lovejoy et al., 1998; Wesselingh et
460 al., 2006). It is unlikely that the ancestral *Hypostomus* lived in this brackish-like lentic habitat,
461 as we found that adaptation to brackish waters occurred only once and recently in the
462 evolutionary history of *Hypostomus*, with *Hypostomus watwata* inhabiting the estuaries of

463 Guianese rivers. Moreover, our habitat preference reconstructions indicate that the ancestral
464 *Hypostomus* was adapted to small rivers with medium-to-fast flowing waters. It is therefore
465 most likely that the first *Hypostomus* was distributed in small rivers draining the slopes of the
466 mountains surrounding Lake Pebas, either on the Andean side or on the slopes of the Purus
467 Arch.

468 According to our biogeographic analysis, the Western Amazon is the main
469 biohydrogeographic region from which most of the dispersal events originated during the
470 early radiation of *Hypostomus* (Figure 7). In total, the Western Amazon accounted for 30% of
471 all the reconstructed dispersal events along the evolutionary history of *Hypostomus*, a
472 proportion only reached by the Paraguay System (~31%). However, when we consider only
473 the first half of the *Hypostomus* radiation period (12.1–6 Ma), the Western Amazon was the
474 dominant center of dispersal, accounting for 60% of these events.

475 We uncovered that Western Amazon was the center of origin of *Hypostomus*, a result
476 that is in agreement with the few available findings on Neotropical fish. In a recent study of
477 Amazonian fish biodiversity, the Western Amazon area has been suggested to be the main
478 geographic region of origination of the Amazonian fish fauna, with a downstream
479 colonization of the lower Amazon basin (Oberdorff et al., 2019). However, this study was
480 geographically restricted to the Amazon basin only. At a wider spatial scale, detailed fish
481 biogeographic analyses revealed that the entire Amazon basin, taken as a single BHG region,
482 was the center of origin and dispersal into other Neotropical basins for the catfish subfamily
483 Hypoptopomatinae (Chiachio, Oliveira, & Montoya-Burgos, 2008) and for the characiform
484 genus *Triportheus* (Mariguela et al., 2016). Recently, a more refined biogeographic
485 reconstruction also revealed the Western Amazon as the origin of marine-derived Neotropical
486 freshwater stingrays (Fontenelle et al., 2021), yet the marine origin of this group may not be
487 representative of other primary freshwater lineages. Therefore, our results bring new evidence

488 in support of the hypothesis that Western Amazon was a primary center of freshwater fish
489 origination.

490 *The role of ecology in Hypostomus dispersal*

491 The preferred ancestral habitat of *Hypostomus* consisted in small-to-medium streams
492 with medium-to-fast flowing waters (Figure 6). This habitat preference predominated in the
493 early evolution of *Hypostomus*, while the colonization of new habitats, such as lakes,
494 floodplains, large rivers and estuaries occurred more recently. According to this eco-
495 evolutionary hypothesis, the first half of the *Hypostomus* radiation was characterized by a
496 strong niche conservatism, which may have played a role on the dispersal and speciation
497 modes of this genus. The preferred ancestral habitat of *Hypostomus* is very common in river
498 headwaters, which are portions of drainages prone to be captured by adjacent basins through
499 evolutionary time. Indeed, the geomorphological history of South America has been marked
500 by many events of headwater captures (James S. Albert et al., 2018; Lavarini, Magalhães
501 Júnior, Oliveira, & Carvalho, 2016; Stokes, Goldberg, & Perron, 2018), their incidence being
502 increased by the active tectonics of this continent and by river meandering and erosion in
503 relatively flat relief in several watershed divides.

504 Relying on our findings of *Hypostomus* ancestral habitat preference and strong niche
505 conservatism along most of their early radiation, we propose that much of the dispersal events
506 into new drainages occurred through the process of headwater captures, promoting range
507 expansion and subsequent allopatric speciation due to geographic isolation. In support of this
508 hypothesis, the results of the ancestral habitat reconstructions indicate that ~61% of dispersal
509 events along the evolution of *Hypostomus* took place in species preferring small or medium
510 rivers with fast-flowing waters (lotic habitats). This is an expected outcome of dispersal by
511 headwater captures, and could hardly be explained by dispersal through alternative

512 environments, such as river delta connections during low sea-level periods (Cardoso &
513 Montoya-Burgos, 2009; A. T. Thomaz, Malabarba, & Knowles, 2017), as the habitat
514 preference of the dispersing species does not match the size of the water body or the stillness
515 of the water found in such environments. The role of headwater captures in dispersal and
516 speciation in South American freshwater fishes has been often suggested, and the
517 hydrogeological hypothesis of diversification (J. I. Montoya-Burgos, 2003) was coined to
518 incorporate this phenomenon. Evidence of headwater captures have been found in drainage
519 boundaries all over Tropical South America, such as among Guianese rivers (e.g. Cardoso &
520 Montoya-Burgos, 2009), between the Amazon Basin and Guianese rivers (Hubert & Renno,
521 2006), between the Amazon and the Orinoco basins (J. G. Lundberg et al., 1998), between the
522 Amazon Basin and the Paraguay System (Hubert & Renno, 2006; J. G. Lundberg et al., 1998;
523 J. I. Montoya-Burgos, 2003; Tagliacollo et al., 2015), between the Upper Paraná and the São
524 Francisco river (Machado, Galetti, & Carnaval, 2018), among Atlantic coastal rivers (M. C. S.
525 L. Malabarba, 1998; Ribeiro, 2006; Roxo et al., 2012), and among many others.

526 However, river headwaters are not always located in mountainous landscapes and
527 temporary connections in basin divides located in flatlands might have also been dispersal
528 routes. For instance, the headwaters of the Guaporé River (Amazon Basin) and Paraguay are
529 located in a flat landscape (around 500 m in altitude) and are regularly interconnected during
530 rainy seasons (Carvalho & Albert, 2011). However, this hypothesis fits better with dispersals
531 later in the radiation of *Hypostomus*, when species shifted their habitat preference for more
532 lentic environments.

533 Every dispersal event into a new basin might have been an ecological opportunity for
534 *Hypostomus* to occupy its preferred habitat, with no congeneric competitors. Although more
535 distant relatives were likely present in the newly colonized basins, we can speculate that a
536 perfect niche overlap between the residing distant relatives and the new *Hypostomus* colonists

537 is unlikely, although our data did not allow us to test this hypothesis. The hypothetical
538 absence of strong competitors in basins colonized for the first time by *Hypostomus* would
539 explain the marked niche conservatism characterizing the early evolutionary history of this
540 genus, a hypothesis that can be tested in future studies.

541 We hypothesize that when basins were colonized for the second time, *Hypostomus*
542 started to shift habitat preference, possibly due to competition between resident and colonist
543 congeneric species. This hypothesis is supported by the finding that *Hypostomus* species
544 started to diversify their habitat preference relatively recently along their evolutionary history,
545 when the new dispersers were invading basins already occupied by congenics. We suggest
546 that the diversity in habitat preference among extant *Hypostomus* species (Figure 6) is most
547 likely the outcome of growing intra-generic competition triggered by the repeated
548 colonization of occupied rivers. According to radiation theory, niche shift is a response to
549 inter-specific competition that allows the co-existence of closely related species, increasing
550 local species-richness (Brew, 1982; Schluter, 2000). Consequently, our findings provide
551 instrumental evidence for explaining the remarkable species richness, species coexistence and
552 the wide distribution range of *Hypostomus* in the Neotropics. The eco-evolution of
553 *Hypostomus* diversity, ecology and distribution may serve as evolutionary model for the
554 entire fish community to which *Hypostomus* belongs, and our results may be informative for
555 understanding the evolutionary history of fish taxa with comparable biological and ecological
556 traits.

557 *Western Amazon as a fish center of dispersal*

558 Elaborating on our findings, we propose that Western Amazon is a center of fish
559 dispersal for five main reasons. (I) It is the center of origin of *Hypostomus*, and this is
560 probably the case for many other species-rich Neotropical fish lineages. (II) Western Amazon

561 is geographically located at the heart of Tropical South America, sharing drainage divides
562 with almost all other main river basins with numerous episodic ichthyologic interchanges
563 through headwater captures. (III) During the Miocene to the present, Western Amazon was
564 the BHG region that had the largest amount of long lasting hydrological interchanged with
565 neighboring basins (Supporting file 3, Table S2). (IV) Western Amazon encompasses the
566 largest Neotropical freshwater system, and is the most fish species-rich BHG region
567 nowadays and was already remarkably rich during the Neogene (John G. Lundberg et al.,
568 2011). Together, these characteristics help to explain why Western Amazon exported
569 repeatedly colonists into its neighboring biogeographic areas all along the evolutionary
570 history of *Hypostomus*. We argue that these characteristics may also be valid for many other
571 Tropical South American fish lineages that had Miocene representative in Western Amazon,
572 as this region acted as a distribution platform, boosting their dispersion throughout
573 Neotropical freshwaters.

574 **Conclusions**

575 In the present work, we assessed the assumption that the Amazon basin was a major
576 center of fish dispersal, spreading new species into neighboring Neotropical river basins from
577 the Miocene to the present. Our detailed time-stratified biogeographic reconstruction of
578 *Hypostomus*, one of the most species-rich genera in the Neotropical Region, indicated that
579 this group emerged in the Western Amazon in the Middle Miocene, when the palaeolandscape
580 was completely different from what we observe nowadays. While new *Hypostomus* species
581 were gradually accumulating in Western Amazon, their ancestral habitat preference enabled
582 them to colonize niches devoid of closely related competitors, and through headwater
583 captures, multiplied the ecological opportunities to spread and diversify into newly colonized
584 basins. Dispersal out of Western Amazon was also boosted by the reconfiguration of the

585 paleo-Amazon-Orinoco watershed, with the disconnection of the Orinoco basin and the
586 junction with Eastern Amazon. The central geographic location of Western Amazon, its
587 longstanding connectivity with other basins, its large extension composed of many sub-basins
588 hosting growing number of species, and the headwater captures spreading *Hypostomus*
589 species in adjacent basins, altogether designate Western Amazon as a center of origin and
590 dissemination for *Hypostomus*. As these characteristics might hold true for many fish lineages
591 with Miocene representatives in Western Amazon, the pattern we observed here for
592 *Hypostomus* may also be valid for a significant fraction of the Neotropical fish diversity.
593 This scenario is supported by the fact that the Western Amazon is an extensive area located at
594 the heart of Tropical South America, with long lasting hydrological connections with
595 neighboring basins, as well as multiple episodic fish exchanges via headwater captures.

596 **Acknowledgments**

597 We thank Margaret Zur and Mary Burrige from the Royal Ontario Museum (Canada) for
598 sample donating (*Hypostomus annectens*), Jaime Sarmiento and Soraya Barrera from the
599 Museo Nacional de Historia Natural, La Paz, for sample sharing, and Mike R. May for
600 RevBayes-related advises. Part of the analyses was performed on the Baobab cluster, a high
601 performance-computing cluster of the University of Geneva. Funding were provided by
602 *Conselho Nacional de Desenvolvimento Científico e Tecnológico*, Brazil (Program Sciences
603 without Borders, CNPq 229237/2013-4, granted to LJQ; CNPq 423526/2018-9 and
604 312801/2017-3, granted to PAB; CNPQ 307775/2018-6 and 424668/2018-1, granted to TEP);
605 Brazilian–Swiss Joint Research Programme, Switzerland (BSJRP S18794, granted to JIMB,
606 GTV and LJQ); *Comissão de Aperfeiçoamento do Pessoal de Nível Superior*, Brazil
607 (CNPq/CAPES 88882.156885/2016-01 granted to PAB); *Donation Claraz*, Switzerland
608 (granted to JIMB); *Fundação Carlos Chagas Filho de Apoio à Pesquisa do Estado do Rio de*

609 *Janeiro* (FAPERJ 200.063/2019 granted to PAB); Swiss Seed Money Grants Latin America
610 2015, Switzerland (granted to JIMB and YPC); Swiss National Science Foundation (SNSF
611 3100A0-104005, granted to JIMB; SNSF P400PB 186777, granted to XM).

612 **References**

613 Abell, R., Thieme, M. L., Revenga, C., Bryer, M., Kottelat, M., Bogutskaya, N., ... Petry, P.
614 (2008). Freshwater Ecoregions of the World: A New Map of Biogeographic Units for
615 Freshwater Biodiversity Conservation. *BioScience*, 58(5), 403–414. doi:
616 10.1641/B580507

617 Albert, J. S., & Carvalho, T. P. (2011). Neogene Assembly of Modern Faunas. In *Historical*
618 *Biogeography of Neotropical Freshwater Fishes* (pp. 119–136). Berkeley, Los
619 Angeles and London: University of California Press. Retrieved from
620 [https://www.researchgate.net/publication/279241320_Continental-](https://www.researchgate.net/publication/279241320_Continental-Scale_Tectonic_Controls_of_Biogeography_and_Ecology)
621 [Scale_Tectonic_Controls_of_Biogeography_and_Ecology](https://www.researchgate.net/publication/279241320_Continental-Scale_Tectonic_Controls_of_Biogeography_and_Ecology)

622 Albert, J. S., & Reis, R. E. (2011). Introduction to Neotropical Freshwaters. In J. Albert & R.
623 E. Reis (Eds.), *Historical Biogeography of Neotropical Freshwater Fishes* (pp. 2–19).
624 Berkeley, Los Angeles and London: University of California Press.

625 Albert, J. S., Val, P., & Hoorn, C. (2018). The changing course of the Amazon River in the
626 Neogene: Center stage for Neotropical diversification. *Neotropical Ichthyology*, 16(3).
627 doi: 10.1590/1982-0224-20180033

628 Antonelli, A., Ariza, M., Albert, J., Andermann, T., Azevedo, J., Bacon, C., ... Edwards, S.
629 V. (2018). Conceptual and empirical advances in Neotropical biodiversity research.
630 *PeerJ*, 6. doi: 10.7717/peerj.5644

631 Antonelli, A., & Sanmartín, I. (2011). Why are there so many plant species in the Neotropics?
632 *TAXON*, 60(2), 403–414. doi: 10.1002/tax.602010

- 633 Antonelli, A., Zizka, A., Carvalho, F. A., Scharn, R., Bacon, C. D., Silvestro, D., &
634 Condamine, F. L. (2018). Amazonia is the primary source of Neotropical biodiversity.
635 *Proceedings of the National Academy of Sciences*, *115*(23), 6034–6039. doi:
636 10.1073/pnas.1713819115
- 637 Baele, G., Lemey, P., & Vansteelandt, S. (2013). Make the most of your samples: Bayes
638 factor estimators for high-dimensional models of sequence evolution. *BMC*
639 *Bioinformatics*, *14*(1), 85. doi: 10.1186/1471-2105-14-85
- 640 Böhlke, J. E., Weitzman, S. H., Menezes, N. A., Böhlke, J. E., Weitzman, S. H., & Menezes,
641 N. A. (1978). Estado atual da sistemática dos peixes de água doce da América do Sul.
642 *Acta Amazonica*, *8*(4), 657–677. doi: 10.1590/1809-43921978084657
- 643 Brew, J. S. (1982). Niche shift and the minimisation of competition. *Theoretical Population*
644 *Biology*, *22*(3), 367–381. doi: 10.1016/0040-5809(82)90050-8
- 645 Cardoso, Y. P., Jardim de Queiroz, L., Bahechar, I. A., Posadas, P. E., & Montoya-Burgos, J.
646 I. (2021). Multilocus phylogeny and historical biogeography of *Hypostomus* shed
647 light on the processes of fish diversification in La Plata Basin. *Scientific Reports*,
648 *11*(1), 5073. doi: 10.1038/s41598-021-83464-x
- 649 Cardoso, Y. P., & Montoya-Burgos, J. I. (2009). Unexpected diversity in the catfish
650 *Pseudancistrus brevispinis* reveals dispersal routes in a Neotropical center of
651 endemism: The Guyanas Region. *Molecular Ecology*, *18*(5), 947–964. doi:
652 10.1111/j.1365-294X.2008.04068.x
- 653 Carvalho, T. P., & Albert, J. S. (2011). The Amazon-Paraguay Divide. In *Historical*
654 *Biogeography of Neotropical Freshwater Fishes* (pp. 193–202). Berkeley: University
655 of California Press. Retrieved from
656 <http://oxfordindex.oup.com/view/10.1525/california/9780520268685.003.0011>,
657 [//oxfordindex.oup.com/view/10.1525/california/9780520268685.003.0011](http://oxfordindex.oup.com/view/10.1525/california/9780520268685.003.0011)

- 658 Chiachio, M. C., Oliveira, C., & Montoya-Burgos, J. I. (2008). Molecular systematic and
659 historical biogeography of the armored Neotropical catfishes Hypoptopomatinae and
660 Neoplecostominae (Siluriformes: Loricariidae). *Molecular Phylogenetics and*
661 *Evolution*, 49(2), 606–617. doi: 10.1016/j.ympev.2008.08.013
- 662 Cox, B. (2001). The biogeographic regions reconsidered. *Journal of Biogeography*, 28(4),
663 511–523. doi: 10.1046/j.1365-2699.2001.00566.x
- 664 Crampton, W. G. R. (2011). An Ecological Perspective on Diversity and Distributions. In J.
665 Albert & R. E. Reis (Eds.), *Historical Biogeography of Neotropical Freshwater*
666 *Fishes* (pp. 165–189). Berkeley, Los Angeles and London: University of California
667 Press.
- 668 Drummond, A. J., Ho, S. Y. W., Phillips, M. J., & Rambaut, A. (2006). Relaxed
669 Phylogenetics and Dating with Confidence. *PLoS Biol*, 4(5), e88. doi:
670 10.1371/journal.pbio.0040088
- 671 Drummond, A. J., & Rambaut, A. (2007). BEAST: Bayesian evolutionary analysis by
672 sampling trees. *BMC Evolutionary Biology*, 7(1), 214. doi: 10.1186/1471-2148-7-214
- 673 Drummond, A. J., Suchard, M. A., Xie, D., & Rambaut, A. (2012a). Bayesian Phylogenetics
674 with BEAUti and the BEAST 1.7. *Molecular Biology and Evolution*, 29(8), 1969–
675 1973. doi: 10.1093/molbev/mss075
- 676 Drummond, A. J., Suchard, M. A., Xie, D., & Rambaut, A. (2012b). Bayesian Phylogenetics
677 with BEAUti and the BEAST 1.7. *Molecular Biology and Evolution*, 29(8), 1969–
678 1973. doi: 10.1093/molbev/mss075
- 679 Duchêne, S., Lanfear, R., & Ho, S. Y. W. (2014). The impact of calibration and clock-model
680 choice on molecular estimates of divergence times. *Molecular Phylogenetics and*
681 *Evolution*, 78, 277–289. doi: 10.1016/j.ympev.2014.05.032

- 682 Evenstar, L. A., Stuart, F. M., Hartley, A. J., & Tattitch, B. (2015). Slow Cenozoic uplift of
683 the western Andean Cordillera indicated by cosmogenic ^3He in alluvial boulders from
684 the Pacific Planation Surface. *Geophysical Research Letters*, *42*(20), 8448–8455. doi:
685 10.1002/2015GL065959
- 686 Fontenelle, J. P., Marques, F. P. L., Kolmann, M. A., & Lovejoy, N. R. (2021). Biogeography
687 of the neotropical freshwater stingrays (Myliobatiformes: Potamotrygoninae) reveals
688 effects of continent-scale paleogeographic change and drainage evolution. *Journal of*
689 *Biogeography*, *n/a*(*n/a*). doi: <https://doi.org/10.1111/jbi.14086>
- 690 Ho, S. Y. W., Tong, K. J., Foster, C. S. P., Ritchie, A. M., Lo, N., & Crisp, M. D. (2015).
691 Biogeographic calibrations for the molecular clock. *Biology Letters*. (world). doi:
692 10.1098/rsbl.2015.0194
- 693 Höhna, S., Landis, M. J., Heath, T. A., Boussau, B., Lartillot, N., Moore, B. R., ... Ronquist,
694 F. (2016). RevBayes: Bayesian Phylogenetic Inference Using Graphical Models and
695 an Interactive Model-Specification Language. *Systematic Biology*, *65*(4), 726–736.
696 doi: 10.1093/sysbio/syw021
- 697 Hoorn, C., Bogotá-A, G. R., Romero-Baez, M., Lammertsma, E. I., Flantua, S. G. A., Dantas,
698 E. L., ... Chemale, F. (2017). The Amazon at sea: Onset and stages of the Amazon
699 River from a marine record, with special reference to Neogene plant turnover in the
700 drainage basin. *Global and Planetary Change*, *153*, 51–65. doi:
701 10.1016/j.gloplacha.2017.02.005
- 702 Hoorn, C., Guerrero, J., Sarmiento, G. A., & Lorente, M. A. (1995). Andean tectonics as a
703 cause for changing drainage patterns in Miocene northern South America. *Geology*,
704 *23*(3), 237–240. doi: 10.1130/0091-7613(1995)023<0237:ATAACF>2.3.CO;2
- 705 Hoorn, C., Wesselingh, F. P., Steege, H. ter, Bermudez, M. A., Mora, A., Sevink, J., ...
706 Antonelli, A. (2010). Amazonia Through Time: Andean Uplift, Climate Change,

- 707 Landscape Evolution, and Biodiversity. *Science*, 330(6006), 927–931. doi:
708 10.1126/science.1194585
- 709 Hubert, N., & Renno, J.-F. (2006). Historical biogeography of South American freshwater
710 fishes. *Journal of Biogeography*, 33(8), 1414–1436. doi: 10.1111/j.1365-
711 2699.2006.01518.x
- 712 Hughes, C. E., Pennington, R. T., & Antonelli, A. (2013). Neotropical Plant Evolution:
713 Assembling the Big Picture. *Botanical Journal of the Linnean Society*, 171(1), 1–18.
714 doi: 10.1111/boj.12006
- 715 Jaramillo, C., Romero, I., D’Apolito, C., Bayona, G., Duarte, E., Louwye, S., ... Wesselingh,
716 F. P. (2017). Miocene flooding events of western Amazonia. *Science Advances*, 3(5),
717 e1601693. doi: 10.1126/sciadv.1601693
- 718 Jardim de Queiroz, L., Cardoso, Y., Jacot-des-Combes, C., Bahechar, I. A., Lucena, C. A.,
719 Rapp Py-Daniel, L., ... Montoya-Burgos, J. I. (2020). Evolutionary units delimitation
720 and continental multilocus phylogeny of the hyperdiverse catfish genus *Hypostomus*.
721 *Molecular Phylogenetics and Evolution*, 145, 106711. doi:
722 10.1016/j.ympev.2019.106711
- 723 Jordan, T. E., Isacks, B. L., Allmendinger, R. W., Brewer, J. A., Ramos, V. A., & Ando, C. J.
724 (1983). Andean tectonics related to geometry of subducted Nazca plate. *GSA Bulletin*,
725 94(3), 341–361. doi: 10.1130/0016-7606(1983)94<341:ATRTGO>2.0.CO;2
- 726 Landis, M. J., Freyman, W. A., & Baldwin, B. G. (2018). Retracing the Hawaiian silversword
727 radiation despite phylogenetic, biogeographic, and paleogeographic uncertainty.
728 *Evolution*, 72(11), 2343–2359. doi: 10.1111/evo.13594
- 729 Lanfear, R., Frandsen, P. B., Wright, A. M., Senfeld, T., & Calcott, B. (2016). PartitionFinder
730 2: New Methods for Selecting Partitioned Models of Evolution for Molecular and

- 731 Morphological Phylogenetic Analyses. *Molecular Biology and Evolution*, 34(3), 772–
732 773. doi: 10.1093/molbev/msw260
- 733 Lavarini, C., Magalhães Júnior, A. P., Oliveira, F. S. de, & Carvalho, A. de. (2016).
734 Neotectonics, river capture and landscape evolution in the highlands of SE Brazil.
735 *Mercator (Fortaleza)*, 15(4), 95–119. doi: 10.4215/rm2016.1504.0007
- 736 Leroy, B., Dias, M. S., Giraud, E., Hugueny, B., Jézéquel, C., Leprieur, F., ... Tedesco, P. A.
737 (2019). Global biogeographical regions of freshwater fish species. *Journal of*
738 *Biogeography*, 46(11), 2407–2419. doi: 10.1111/jbi.13674
- 739 Lévêque, C., Oberdorff, T., Paugy, D., Stiassny, M. L. J., & Tedesco, P. A. (2008). Global
740 diversity of fish (Pisces) in freshwater. In E. V. Balian, C. Lévêque, H. Segers, & K.
741 Martens (Eds.), *Freshwater Animal Diversity Assessment* (pp. 545–567). Dordrecht:
742 Springer Netherlands. doi: 10.1007/978-1-4020-8259-7_53
- 743 Lovejoy, N. R., Bermingham, E., & Martin, A. P. (1998). Marine incursion into South
744 America. *Nature*, 396(6710), 421–422. doi: 10.1038/24757
- 745 Lundberg, J. G., Marshall, L. G., Guerrero, J., Horton, B., Malabarba, L. M. C. S., &
746 Wesselingh, F. (1998). The stage for neotropical fish diversification: A history of
747 tropical South American rivers. In L. R. Malabarba, R. E. Reis, R. Vari, L. C. A.
748 Lucena, & Z. M. S. Lucena (Eds.), *Phylogeny and Classification of Neotropical*
749 *Fishes* (pp. 13–48). Porto Alegre: EDIPUCRS.
- 750 Lundberg, J. G., Pérez, M. H. S., Dahdul, W. M., & Aguilera, O. A. (2011). The Amazonian
751 Neogene Fish Fauna. In *Amazonia: Landscape and Species Evolution* (pp. 281–301).
752 John Wiley & Sons, Ltd. doi: 10.1002/9781444306408.ch17
- 753 Machado, C. B., Galetti, P. M., & Carnaval, A. C. (2018). Bayesian analyses detect a history
754 of both vicariance and geodispersal in Neotropical freshwater fishes. *Journal of*
755 *Biogeography*, 45(6), 1313–1325. doi: 10.1111/jbi.13207

- 756 Malabarba, M. C. S. L. (1998). Phylogeny of Fossil Characiformes and Paleobiogeography of
757 the Tremembé Formation, São Paulo, Brazil. In *Phylogeny and Classification of*
758 *Neotropical Fishes* (pp. 69–84). Porto Alegre: PUCRS.
- 759 Mariguela, T. C., Roxo, F. F., Foresti, F., & Oliveira, C. (2016). Phylogeny and biogeography
760 of Triportheidae (Teleostei: Characiformes) based on molecular data. *Molecular*
761 *Phylogenetics and Evolution*, 96, 130–139. doi: 10.1016/j.ympev.2015.11.018
- 762 Montoya-Burgos, J. I. (2003). Historical biogeography of the catfish genus *Hypostomus*
763 (Siluriformes: Loricariidae), with implications on the diversification of Neotropical
764 ichthyofauna. *Molecular Ecology*, 12(7), 1855–1867. doi: 10.1046/j.1365-
765 294X.2003.01857.x
- 766 Musher, L. J., Ferreira, M., Auerbach, A. L., McKay, J., & Cracraft, J. (2019). Why is
767 Amazonia a ‘source’ of biodiversity? Climate-mediated dispersal and synchronous
768 speciation across the Andes in an avian group (Tityrinae). *Proceedings of the Royal*
769 *Society B: Biological Sciences*, 286(1900), 20182343. doi: 10.1098/rspb.2018.2343
- 770 Oberdorff, T., Dias, M. S., Jézéquel, C., Albert, J. S., Arantes, C. C., Bigorne, R., ... Zuanon,
771 J. (2019). Unexpected fish diversity gradients in the Amazon basin. *Science Advances*,
772 5(9), eaav8681. doi: 10.1126/sciadv.aav8681
- 773 Pilger, R. H. (1984). Cenozoic plate kinematics, subduction and magmatism: South American
774 Andes. *Journal of the Geological Society*, 141(5), 793–802. doi:
775 10.1144/gsjgs.141.5.0793
- 776 Ree, R. H., Moore, B. R., Webb, C. O., Donoghue, M. J., & Crandall, K. (2005). A likelihood
777 framework for inferring the evolution of geographic range on phylogenetic trees.
778 *Evolution*, 59(11), 2299–2311. doi: 10.1554/05-172.1

- 779 Ree, R. H., & Smith, S. A. (2008). Maximum Likelihood Inference of Geographic Range
780 Evolution by Dispersal, Local Extinction, and Cladogenesis. *Systematic Biology*,
781 57(1), 4–14. doi: 10.1080/10635150701883881
- 782 Reis, R. E., Kullander, S. O., & Ferraris, C. J. (2003). *Check List of the Freshwater Fishes of*
783 *South and Central America*. EDIPUCRS.
- 784 Ribeiro, A. C. (2006). Tectonic history and the biogeography of the freshwater fishes from
785 the coastal drainages of eastern Brazil: An example of faunal evolution associated
786 with a divergent continental margin. *Neotropical Ichthyology*, 4(2), 225–246. doi:
787 10.1590/S1679-62252006000200009
- 788 Roxo, F. F., Albert, J. S., Silva, G. S. C., Zawadzki, C. H., Foresti, F., & Oliveira, C. (2014).
789 Molecular Phylogeny and Biogeographic History of the Armored Neotropical Catfish
790 Subfamilies Hypoptopomatinae, Neoplecostominae and Otothyriinae (Siluriformes:
791 Loricariidae). *PLOS ONE*, 9(8), e105564. doi: 10.1371/journal.pone.0105564
- 792 Roxo, F. F., Zawadzki, C. H., Alexandrou, M. A., Costa Silva, G. J., Chiachio, M. C., Foresti,
793 F., & Oliveira, C. (2012). Evolutionary and biogeographic history of the subfamily
794 Neoplecostominae (Siluriformes: Loricariidae). *Ecology and Evolution*, 2(10), 2438–
795 2449. doi: 10.1002/ece3.368
- 796 Schluter, D. (2000). Ecological Character Displacement in Adaptive Radiation. *The American*
797 *Naturalist*, 156(S4), S4–S16. doi: 10.1086/303412
- 798 Silva, G. S. C., Roxo, F. F., Lujan, N. K., Tagliacollo, V. A., Zawadzki, C. H., & Oliveira, C.
799 (2016). Transcontinental dispersal, ecological opportunity and origins of an adaptive
800 radiation in the Neotropical catfish genus *Hypostomus* (Siluriformes: Loricariidae).
801 *Molecular Ecology*, 25(7), 1511–1529. doi: 10.1111/mec.13583
- 802 Stokes, M. F., Goldberg, S. L., & Perron, J. T. (2018). Ongoing River Capture in the Amazon.
803 *Geophysical Research Letters*, 45(11), 5545–5552. doi: 10.1029/2018GL078129

- 804 Tagliacollo, V. A., Roxo, F. F., Duke-Sylvester, S. M., Oliveira, C., & Albert, J. S. (2015).
805 Biogeographical signature of river capture events in Amazonian lowlands. *Journal of*
806 *Biogeography*, 2349–2362. doi: 10.1111/jbi.12594
- 807 Thomaz, A. T., Malabarba, L. R., & Knowles, L. L. (2017). Genomic signatures of
808 paleodrainages in a freshwater fish along the southeastern coast of Brazil: Genetic
809 structure reflects past riverine properties. *Heredity*, 119(4), 287–294. doi:
810 10.1038/hdy.2017.46
- 811 Vari, R. P. (1988). The Curimatidae, a lowland neotropical fish family (Pisces:
812 Characiformes): distribution, endemism, and phylogenetic biogeography. *Neotropical*
813 *Distribution Patterns: Proceedings of a Workshop*. Rio de Janeiro: Academia
814 *Brasileira de Ciencias.*, 343–377.
- 815 Wendt, E. W., Silva, P. C., Malabarba, L. R., & Carvalho, T. P. (2019). Phylogenetic
816 relationships and historical biogeography of *Oligosarcus* (Teleostei: Characidae):
817 Examining riverine landscape evolution in southeastern South America. *Molecular*
818 *Phylogenetics and Evolution*, 140, 106604. doi: 10.1016/j.ympev.2019.106604
- 819 Wesselingh, F. P., Guerrero, J., Rasanen, M. E., Romero Pittman, L., & Vonhof, H. B. (2006).
820 Landscape evolution and depositional processes in the Miocene Amazonian Pebas
821 lake/wetland system: Evidence from exploratory boreholes in northeastern Peru.
822 *Instituto Geológico, Minero y Metalúrgico – INGEMMET*. Retrieved from
823 <http://repositorio.ingemmet.gob.pe/handle/ingemmet/664>

824

825 **Data Availability Statement**

826 The new DNA sequences used in this study are available from the NCBI

827 (Supporting file 3, Table S3). Complete concatenated alignment (except new sequences
828 generated in the present work) is available from Jardim de Queiroz and colleagues (Jardim de
829 Queiroz et al., 2020) DOI: 10.17632/wccvm8p5gx.1. XML files to reconstruct and calibrate
830 the phylogeny, and to reconstruct habitat preference are available from Supporting file 1.
831 Custom codes used to reconstruct the biogeography with RevBayes are available from
832 Supporting file 2 and from the GIT repository
833 <https://bitbucket.org/XavMeyer/biogeographyrevscript/src/master/>.

834 **Author Contribution**

835 LJQ and JIMB designed the research, analyzed and interpreted the results and drafted the
836 manuscript. LJQ assembled the data and ran the analyses. IAB conducted part of the wet-
837 laboratory routine. XM wrote the helper script specifying RevBayes analyses, helped to run
838 the biogeographic analyses and to interpret the results. YC, RC, GTV, TEP and PAB
839 provided samples and/or laboratorial infrastructure to generate part of the data. All authors
840 read, contributed to the content and approved the final version.

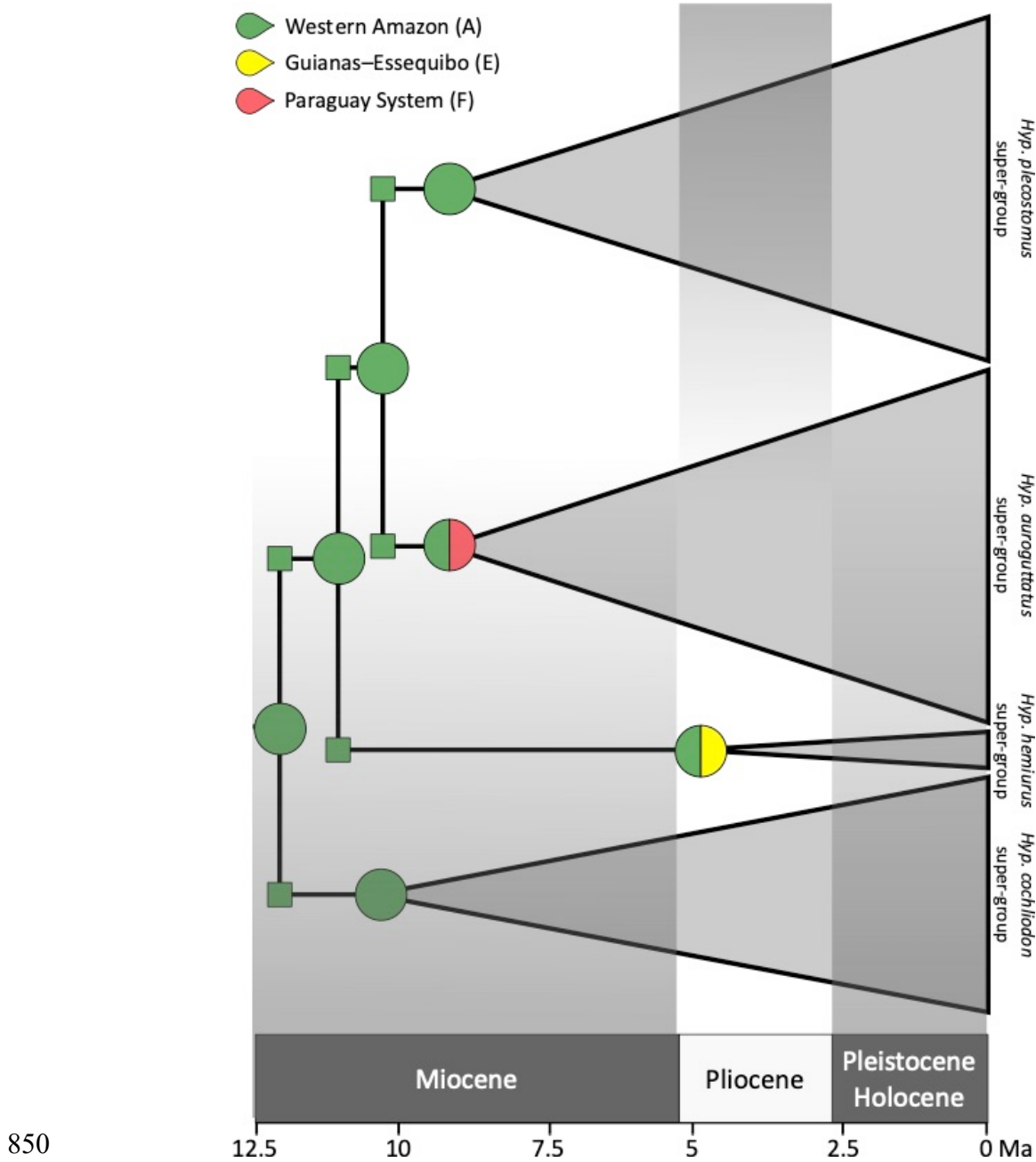
841

842 Table 1. Retrieved ages and Highest Posterior Density (HPD) 95% (between brackets) of six representative
 843 nodes of the *Hypostomus* phylogenetic tree. Four calibration analyses were performed (Supporting file 1). In
 844 *scenario 1*, from which the results of this work are based on, all four-calibration points were used as priors; in
 845 *scenario 2*, the calibration point 3 (Tocantins–Amazon disconnection) was not included; in *scenario 3*, the
 846 calibration point 4 (Amazon–Pilcomayo headwater capture) was not included; and in *scenario 4*, calibration
 847 point 2 (Uplift of Ecuadorian Andes) was not included. MRCA: most recent common ancestor.

Node	Biogeographical event and age	Scenario 1	Scenario 2	Scenario 3	Scenario 4
Origin of <i>Hypostomus</i> + closest relatives	–	14.7 [17.8–11.4]	14.6 [17.7–11.7]	14.8 [18.0–12.0]	20.3 [27.4–14.2]
<i>Hemiancistrus</i>	–	12.1 [14.3–10.1]	12.1 [14.4–10.0]	12.2 [14.5–10.2]	16.3 [21.6–11.8]
<i>Hypostomus</i> MRCA	–	12.1 [14.3–10.1]	12.1 [14.4–10.0]	12.2 [14.5–10.2]	16.3 [21.6–11.8]
Calibration point 1: <i>Hyp. hondae</i> + <i>Hyp. plecostomoides</i>	Uplift of Cordillera de Mérida (8 Ma)	7.3 [7.9–7.0]	7.3 [7.9–7.0]	7.4 [7.9–7.0]	7.7 [8.6–7.0]
Calibration point 2: <i>Isorineloricaria</i> + <i>Aphanotorlus</i>	Uplift of Ecuadorian Andes (10 Ma)	10.8 [12.0–9.8]	10.9 [12.0–9.8]	10.9 [12.0–9.8]	19.6 [27.3–13.0]
Calibration point 3: <i>Hyp. sp.'xin2'</i> + <i>Hyp. sp.'Tar'</i>	Tocantins–Amazon disconnection (3.6–1.8 Ma)	2.6 [3.9–1.3]	2.7 [4.8–1.0]	2.6 [5.3–1.3]	3.0 [4.4–1.9]
Calibration point 4: <i>Hyp. cf. borelli</i> + <i>Hyp. sp.'Rio Grande'</i>	Amazon–Pilcomayo headwater capture (~1 Ma)	1.2 [1.7–0.6]	1.2 [1.7–0.7]	1.3 [2.0–0.7]	1.5 [2.3–0.8]

848

849



850

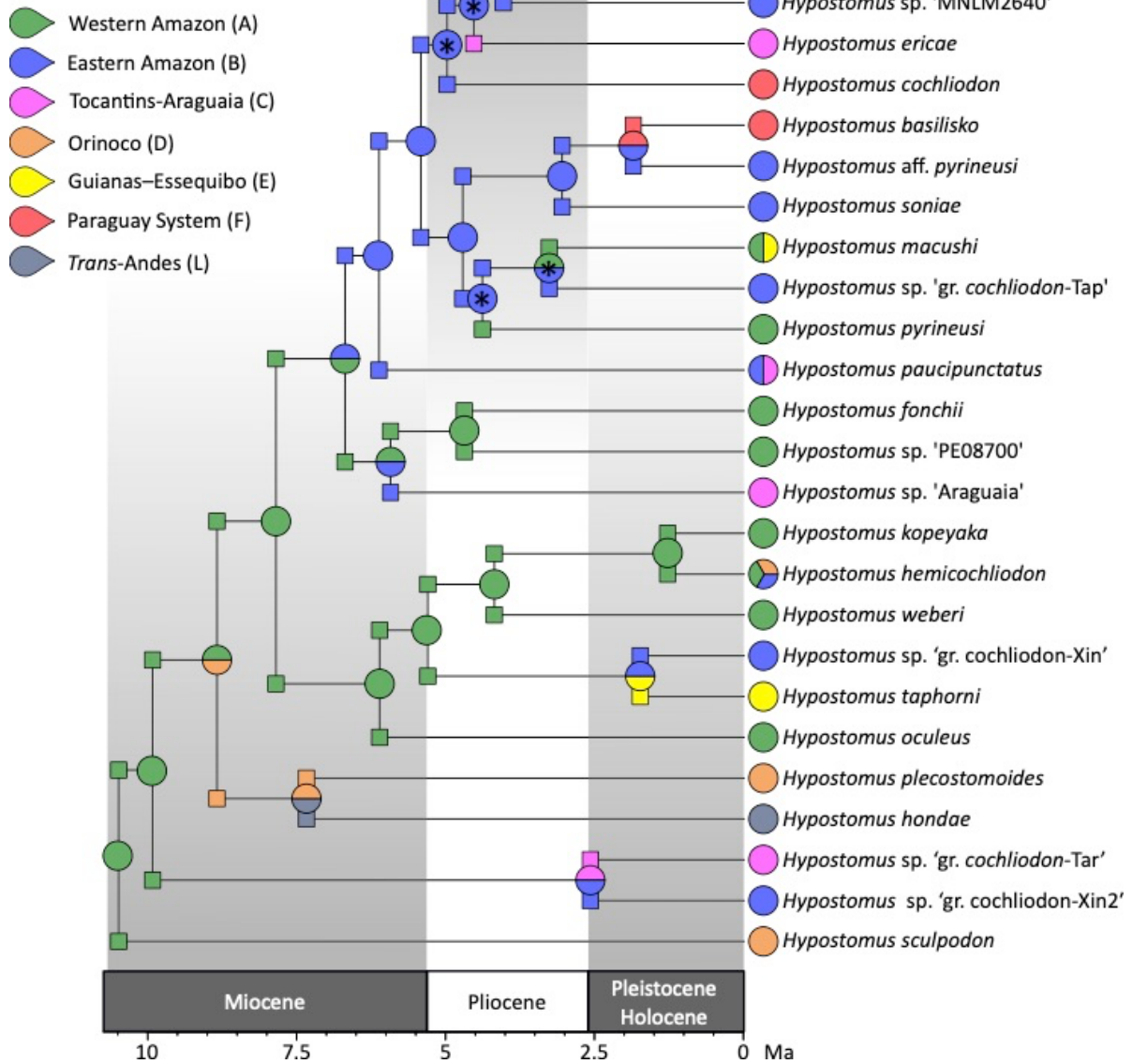
851 Figure 1 Ancestral range reconstruction of the first ancestral *Hypostomus* and of the ancestors of the four main

852 internal lineages. For detailed results, see Figs. 2–5. The posterior probabilities of the ancestral range

853 reconstructions shown here are ≥ 0.55 .

854

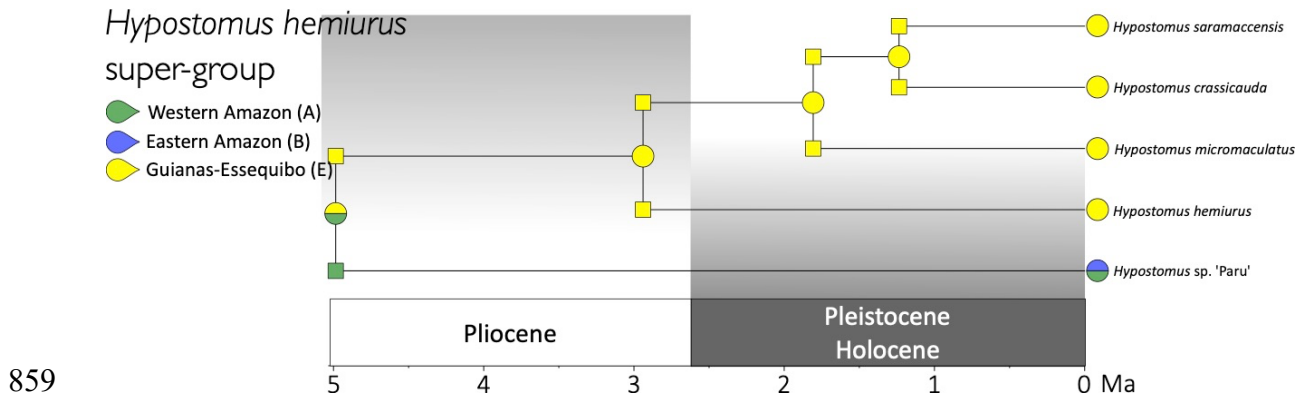
Hypostomus cochliodon super-group



855

856 Figure 2 Ancestral range reconstruction of the *Hypostomus cochliodon* super-group. (* posterior probability of
857 ancestral range reconstruction < 0.5).

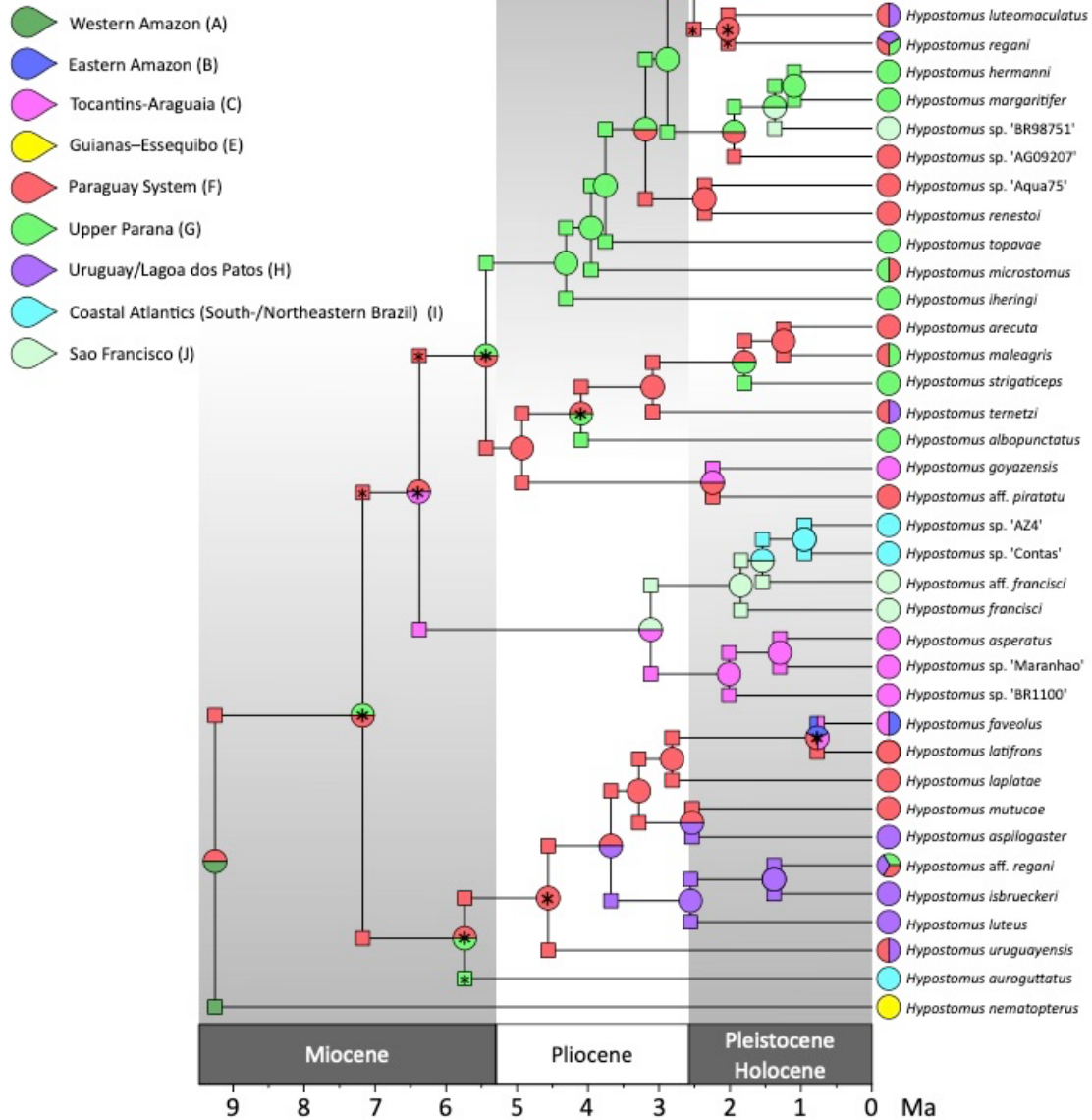
858



860 Figure 3 Ancestral range reconstruction of the *Hypostomus hemiurus* super-group. The posterior probabilities of
861 ancestral range reconstructions shown here are ≥ 0.54).

Hypostomus auroguttatus

super-group (+ *Hyp. nematopterus*)

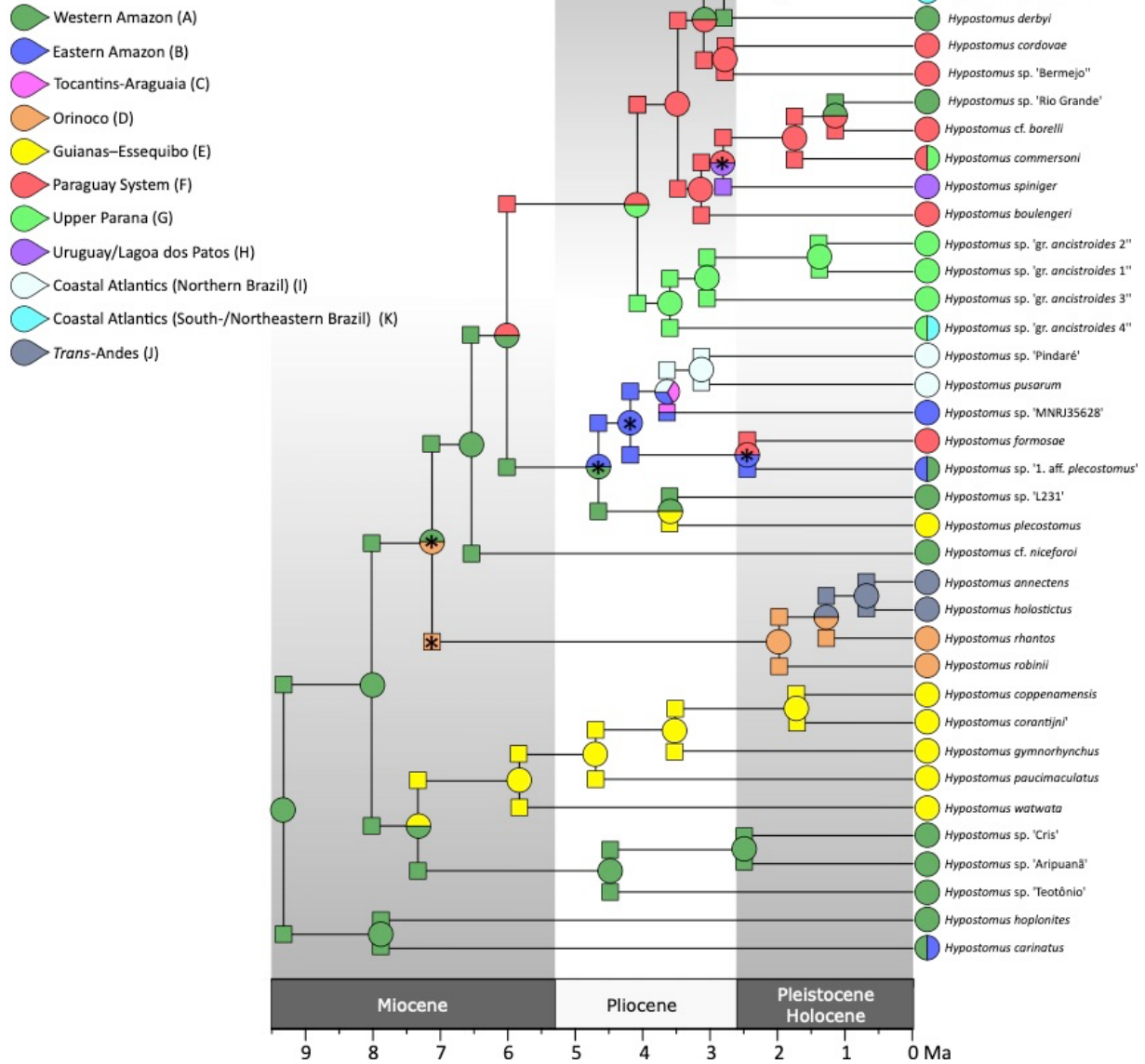


862

863 Figure 4 Ancestral range reconstruction of the clade that contains the *Hypostomus auroguttatus* super-group and

864 *Hypostomus nematopterus*. (* posterior probability of ancestral range reconstruction < 0.5).

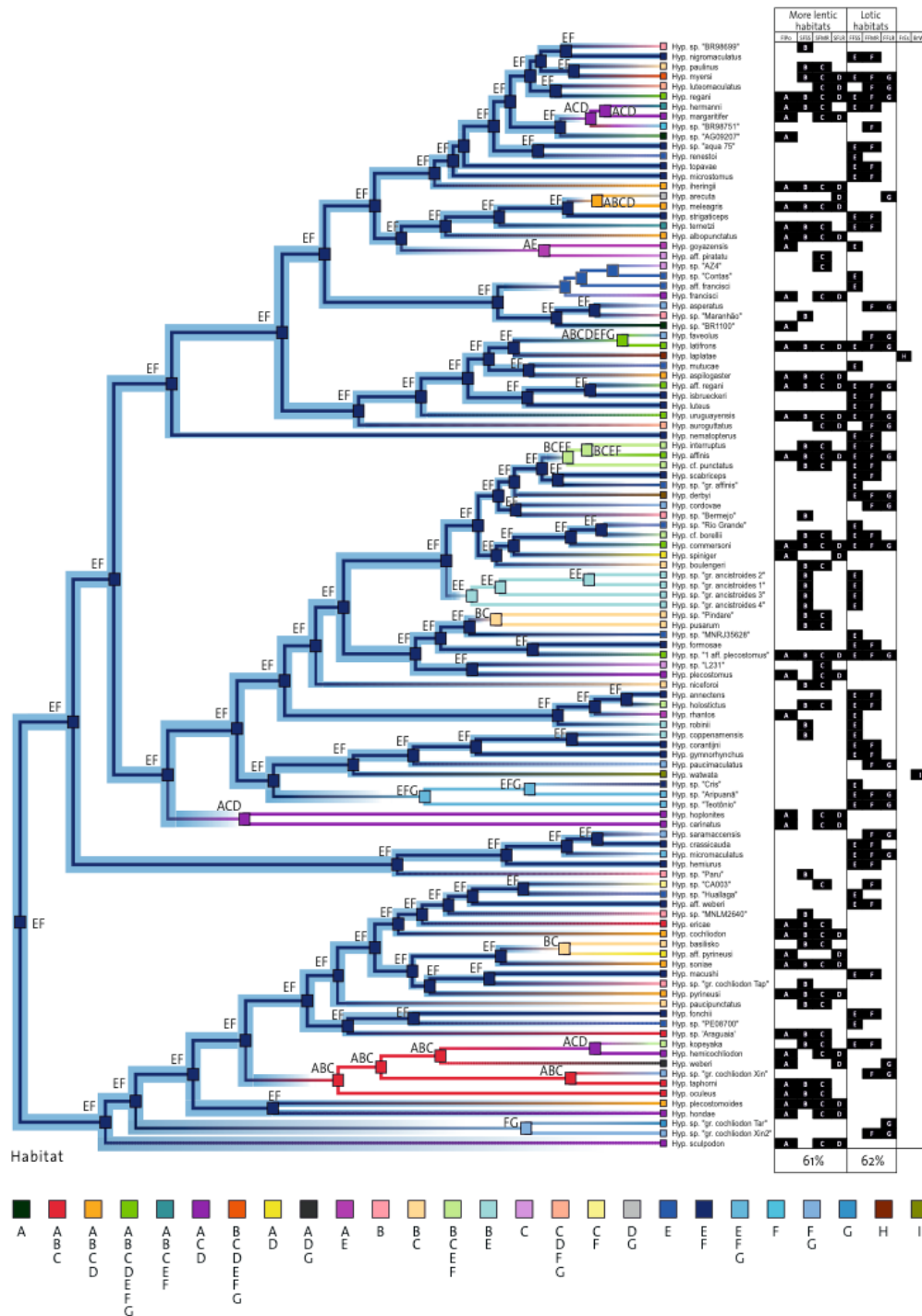
Hypostomus plecostomus super-group



865

866 Figure 5 Ancestral range reconstruction of the *Hypostomus plecostomus* super-group. (* posterior probability of
867 ancestral range reconstruction < 0.5).

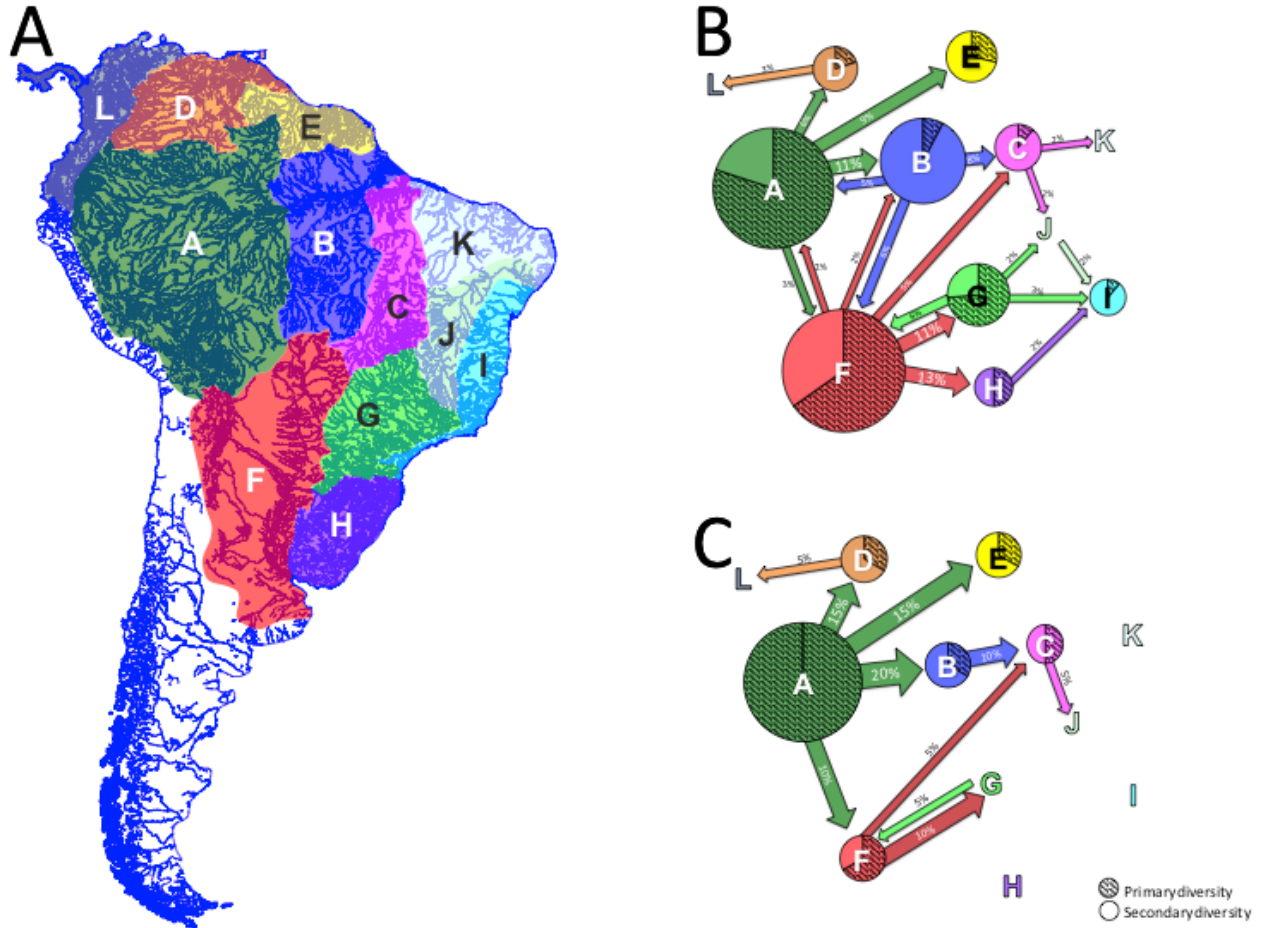
868



869

870 Figure 6 Ancestral habitat reconstruction of *Hypostomus*. A = floodplains and ponds (FIPo); B = slow flowing
 871 small streams (SFSS); C = slow flowing medium rivers (SFMR); D = Slow flowing large rivers (SFLR); E =
 872 medium to fast flowing small stream (FFSS); F = medium to fast flowing medium rivers (FFMR); G = medium

873 to fast flowing large rivers (FFLR); H = freshwater estuarine systems (FrEs); I = brackish water (BrWa). More
 874 information, including habitat reconstruction of outgroups and posterior probabilities can be found in Supporting
 875 file 1.



876
 877 Figure 7 Dispersal events between biohydrogeographic regions (BHG). A) Map showing the division of South
 878 America into BHG regions. B) Dispersal events inferred from 12.1 Ma to the present. C) Dispersal events
 879 inferred from 12.1 to 6 Ma. Circle sizes are proportional to the number of extant *Hypostomus* species. Dashed
 880 areas of the circles represent "primary diversity", i.e. the proportion of *Hypostomus* species that originated from
 881 the first colonization of the region. Species that arose from secondary colonization events were considered as
 882 "secondary diversity". As the Western Amazon (region A) was the place where *Hypostomus* originated, we
 883 considered as primary diversity only the species that showed no ancestor distributed in another BHG region.
 884

885 **Supporting information (doi:10.17632/2fh5rj2zvg.1)**

886 **Supporting file 1:** XML files for phylogenetic inference and tree calibration, and resulting
887 trees in nexus format. These files correspond to four different runs (four scenarios as
888 described in Table 1 in the main article). XML file for ancestral habitat reconstruction and
889 resulting tree in nexus format are also available.

890 **Supporting file 2:** RevBayes scripts that were modified to constraint a given list of
891 geographic ranges.

892 **Supporting file 3. Tables S1–S3. Table S1.** Marginal likelihoods obtained from the distinct
893 analyses conducted with RevBayes to reconstruct ancestral ranges. **Table S2.**
894 Biohydrogeographic regions and their connectivity through time periods, according to our
895 time-stratified model (M3). **Table S3.** Accession numbers of sequences generated in the
896 present work.